

This is a repository copy of *Aldehyde-mediated protein-to-surface tethering via controlled diazonium electrode functionalization using protected hydroxylamines*.

White Rose Research Online URL for this paper:

<https://eprints.whiterose.ac.uk/156673/>

Version: Accepted Version

---

**Article:**

Yates, Nick, Dowsett, Mark, Bentley, Phillip et al. (5 more authors) (2019) Aldehyde-mediated protein-to-surface tethering via controlled diazonium electrode functionalization using protected hydroxylamines. *Langmuir*. ISSN 1520-5827

<https://doi.org/10.1021/acs.langmuir.9b01254>

---

**Reuse**

Items deposited in White Rose Research Online are protected by copyright, with all rights reserved unless indicated otherwise. They may be downloaded and/or printed for private study, or other acts as permitted by national copyright laws. The publisher or other rights holders may allow further reproduction and re-use of the full text version. This is indicated by the licence information on the White Rose Research Online record for the item.

**Takedown**

If you consider content in White Rose Research Online to be in breach of UK law, please notify us by emailing [eprints@whiterose.ac.uk](mailto:eprints@whiterose.ac.uk) including the URL of the record and the reason for the withdrawal request.

Interfaces: Adsorption, Reactions, Films, Forces, Measurement Techniques, Charge Transfer, Electrochemistry, Electrocatalysis, Energy Production and Storage

## Aldehyde-mediated protein-to-surface tethering via controlled diazonium electrode functionalization using protected hydroxylamines

Nicholas David James Yates, Mark R Dowsett, Phillip Bentley, Jack A Dickenson-Fogg, Andrew Pratt, Christopher Francis Blanford, Martin Fascione, and Alison Parkin

*Langmuir*, **Just Accepted Manuscript** • DOI: 10.1021/acs.langmuir.9b01254 • Publication Date (Web): 13 Nov 2019

Downloaded from [pubs.acs.org](https://pubs.acs.org) on February 7, 2020

### Just Accepted

“Just Accepted” manuscripts have been peer-reviewed and accepted for publication. They are posted online prior to technical editing, formatting for publication and author proofing. The American Chemical Society provides “Just Accepted” as a service to the research community to expedite the dissemination of scientific material as soon as possible after acceptance. “Just Accepted” manuscripts appear in full in PDF format accompanied by an HTML abstract. “Just Accepted” manuscripts have been fully peer reviewed, but should not be considered the official version of record. They are citable by the Digital Object Identifier (DOI®). “Just Accepted” is an optional service offered to authors. Therefore, the “Just Accepted” Web site may not include all articles that will be published in the journal. After a manuscript is technically edited and formatted, it will be removed from the “Just Accepted” Web site and published as an ASAP article. Note that technical editing may introduce minor changes to the manuscript text and/or graphics which could affect content, and all legal disclaimers and ethical guidelines that apply to the journal pertain. ACS cannot be held responsible for errors or consequences arising from the use of information contained in these “Just Accepted” manuscripts.

1  
2  
3  
4  
5  
6  
7 Aldehyde-mediated protein-to-surface tethering via  
8  
9  
10  
11 controlled diazonium electrode functionalization  
12  
13  
14  
15 using protected hydroxylamines  
16  
17  
18  
19

20 *Nicholas D. Yates,<sup>1</sup> Mark R. Dowsett,<sup>1</sup> Phillip Bentley,<sup>2</sup> Jack A. Dickenson-Fogg,<sup>1</sup> Andrew*  
21 *Pratt,<sup>2</sup> Christopher F. Blanford,<sup>3</sup> Martin A. Fascione,<sup>1,\*</sup> and Alison Parkin<sup>1,\*</sup>*  
22  
23  
24  
25

26 1. Department of Chemistry, University of York, Heslington, York, YO10 5DD, United  
27  
28 Kingdom  
29

30  
31 2. Department of Physics, University of York, Heslington, York, YO10 5DD, United  
32  
33 Kingdom  
34  
35

36  
37 3. School of Materials, University of Manchester, Oxford Road, Manchester, M13 9PL,  
38  
39 United Kingdom  
40

41  
42 4. Manchester Institute of Biotechnology, University of Manchester, 131 Princess Street,  
43  
44 Manchester, M1 7DN, United Kingdom  
45  
46

47  
48  
49  
50  
51 \*E-mail [martin.fascione@york.ac.uk](mailto:martin.fascione@york.ac.uk), [alison.parkin@york.ac.uk](mailto:alison.parkin@york.ac.uk).  
52  
53  
54  
55  
56  
57  
58  
59  
60

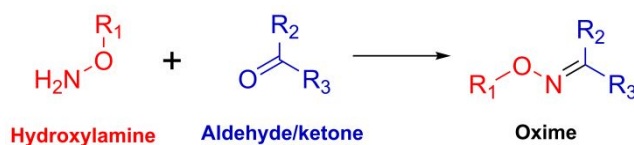
1  
2  
3 ABSTRACT. We report a diazonium electro-grafting method for the covalent modification of  
4  
5 conducting surfaces with aldehyde-reactive hydroxylamine functionalities that facilitate the wiring  
6  
7 of redox-active (bio)molecules to electrode surfaces. Hydroxylamine near-monolayer formation is  
8  
9 achieved via a phthalimide-protection and hydrazine-deprotection strategy that overcomes the  
10  
11 multilayer formation that typically complicates diazonium surface modification. This surface  
12  
13 modification strategy is characterized using electrochemistry (electrochemical impedance  
14  
15 spectroscopy and cyclic voltammetry), X-ray photoelectron spectroscopy and quartz crystal  
16  
17 microbalance with dissipation monitoring. Thus-modified glassy carbon, boron-doped diamond  
18  
19 and gold surfaces are all shown to ligate to small molecule aldehydes, yielding surface coverages  
20  
21 of 150-170, 40 and 100 pmol cm<sup>-2</sup>, respectively. Bio-conjugation is demonstrated via the coupling  
22  
23 of a dilute (50 μM) solution of periodate-oxidized horseradish peroxidase enzyme to a  
24  
25 functionalized gold surface under bio-compatible conditions (H<sub>2</sub>O solvent, pH 4.5, 25 °C).  
26  
27  
28  
29  
30  
31  
32  
33  
34

## 35 INTRODUCTION

36  
37  
38 There is an ever-growing chemical biology toolkit of methodologies for site-selective bio-  
39  
40 orthogonal ligations to proteins, meaning covalent bond formation reactions that target  
41  
42 functionalities which are orthogonal to those which occur in Nature.<sup>1-3</sup> However, a relatively small  
43  
44 number of these methodologies have been converted into robust strategies for immobilizing  
45  
46 proteins onto a wide range of solid substrates.<sup>4-5</sup> This is despite the need for protein immobilization  
47  
48 in industrial biocatalysis, medical diagnostics, tissue culturing, environmental sensing and  
49  
50 biophysical characterisation.<sup>5-7</sup> By developing a procedure that enables the functionalization of a  
51  
52 wide range of solid substrates with near-monolayers of hydroxylamine, we enable the tethering of  
53  
54  
55  
56  
57  
58  
59  
60

1  
2  
3 aldehyde-containing (bio)molecules to solid-substrates via oxime bond formation. We illustrate  
4 the utility of this method with the immobilization of an aldehyde-functionalized horseradish  
5 peroxidase on a hydroxylamine-modified gold electrode surface. The redox-activity of this  
6 enzyme<sup>8-9</sup> enables us to detect its presence on gold surfaces via electrochemistry, while quartz  
7 crystal microbalance with dissipation monitoring probes the change in mass of the electrode  
8 surface throughout the deprotection and protein-coupling process.  
9  
10  
11  
12  
13  
14  
15  
16  
17

18 **Scheme 1.** The ligation of a hydroxylamine to an aldehyde or ketone to form an oxime.  
19  
20



An oxime bond is formed via reaction between an organic hydroxylamine and an aldehyde or a ketone (Scheme 1).<sup>10</sup> It is such a robust and reliable reaction that it has been described as “Click” chemistry.<sup>11</sup> In the protein-immobilization strategy described here, we introduce a hydroxylamine group onto the solid substrate and react this with a protein aldehyde. It is advantageous to design a protein-immobilization strategy that targets aldehydes because there are a wide range of robust methodologies which will introduce these bio-orthogonal carbonyl functionalities into proteins, as shown in Figure 1.<sup>10, 12-14</sup>

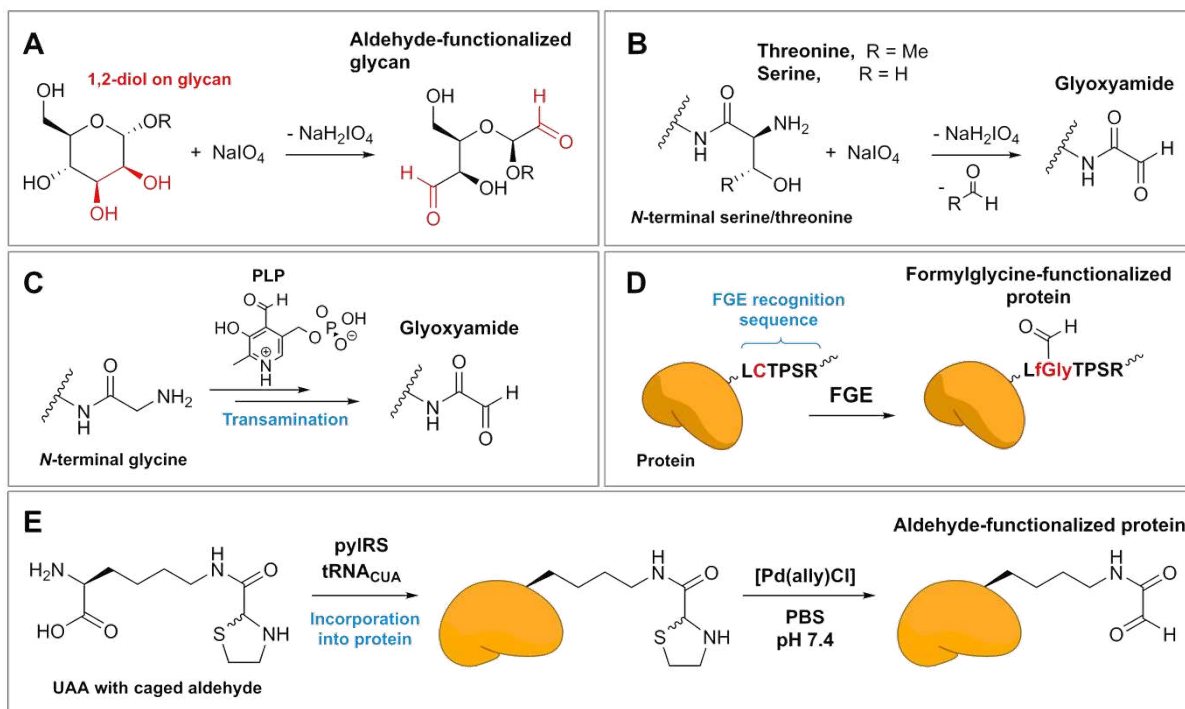


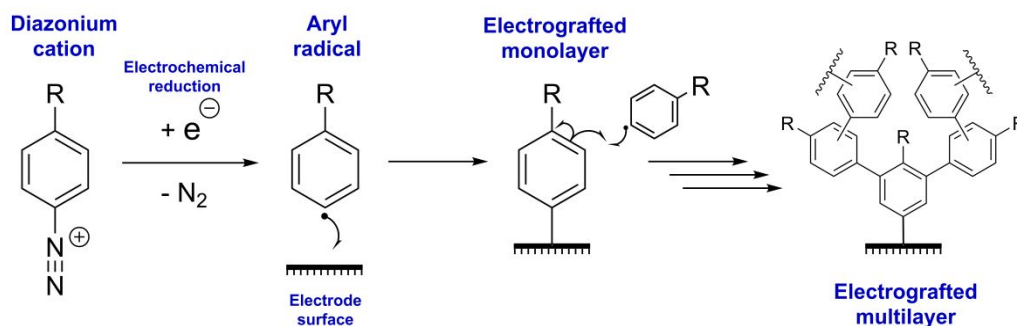
**Figure 1.** Summary of the variety of methods via which aldehyde motifs can be introduced into protein structures. (A) The oxidation of a glycan presenting a cis-1,2 diol with sodium periodate. (B) The oxidation of a 1,2-amino alcohol, such as *N*-terminal serine or threonine residues, with sodium periodate. (C) Pyridoxal 5'-phosphate (PLP) mediated transamination of *N*-terminal glycine residues. (D) Post-translational modification of a pre-installed recognition sequence by a formyl glycine generating enzyme. (E) Unnatural amino acid installation and manipulation.

In the case of glycoproteins, the chemical oxidation of glycans with sodium periodate is a simple way to generate aldehydes (Figure 1A).<sup>10, 15</sup> This is exemplified (*vide infra*) through the use of horseradish peroxidase, a redox-active heme-containing enzyme which presents glycan moieties that can be oxidized to bear aldehydes.<sup>16-18</sup> Proteins that are recombinantly produced in *E. coli* lack such glycosylation, instead they can be site-selectively modified to contain an aldehyde residue by a diverse range of methods including oxidation of an appropriate *N*-terminal amino acid residue

1  
2  
3 (Figure 1B and C),<sup>10, 14</sup> *in vivo* or *in vitro* post-translational modification of a pre-installed  
4 recognition sequence by a formylglycine generating enzyme (Figure 1D),<sup>10, 12, 14</sup> or unnatural  
5 amino acid installation (Figure 1E).<sup>13, 19</sup>  
6  
7  
8  
9

10  
11 Prior to forming an oxime bond between a surface and a protein aldehyde, the solid substrate  
12 must first be decorated with hydroxylamine functionalities. This has previously been performed  
13 using long polymeric linkers on silicon.<sup>20</sup> However, the surface modification chemistry is not  
14 applicable to a broad substrate scope. Gold surfaces have also been functionalized via the  
15 formation of self-assembled monolayers using alkanethiol molecules capped with hydroxylamine  
16 groups.<sup>21</sup> Such a method cannot be translated to the multitude of different solid-materials which  
17 do not form stable surface-thiol bonds,<sup>5</sup> and gold-thiol bonds are not stable with respect to the  
18 application of potentials more negative than -0.9 vs SHE,<sup>22</sup> meaning such surfaces cannot be  
19 utilized in enzyme-catalyzed biofuel-production applications.<sup>5</sup> In contrast, the reduction of aryl  
20 diazonium salts is a widely adopted strategy for introducing chemical functional groups onto  
21 surfaces.<sup>23-24</sup> Indeed, diazonium modification has even been used for protein-surface attachment,  
22 although only via non-oxime ligation strategies.<sup>25-28</sup> The broad utility of diazonium surface-  
23 modification originates from the fact it generates a stable carbon-to-surface covalent bond on a  
24 large variety of different substrates, ranging from semi-conductors (e.g. silicon,<sup>23-24</sup> boron-doped  
25 diamond (BDD)),<sup>29</sup> to metals (e.g. gold),<sup>23-24</sup> other metallic conductors (e.g. graphite),<sup>23-24</sup> and  
26 dielectrics<sup>23-24</sup> (Scheme 2).  
27  
28  
29  
30  
31  
32  
33  
34  
35  
36  
37  
38  
39  
40  
41  
42  
43  
44  
45  
46  
47  
48

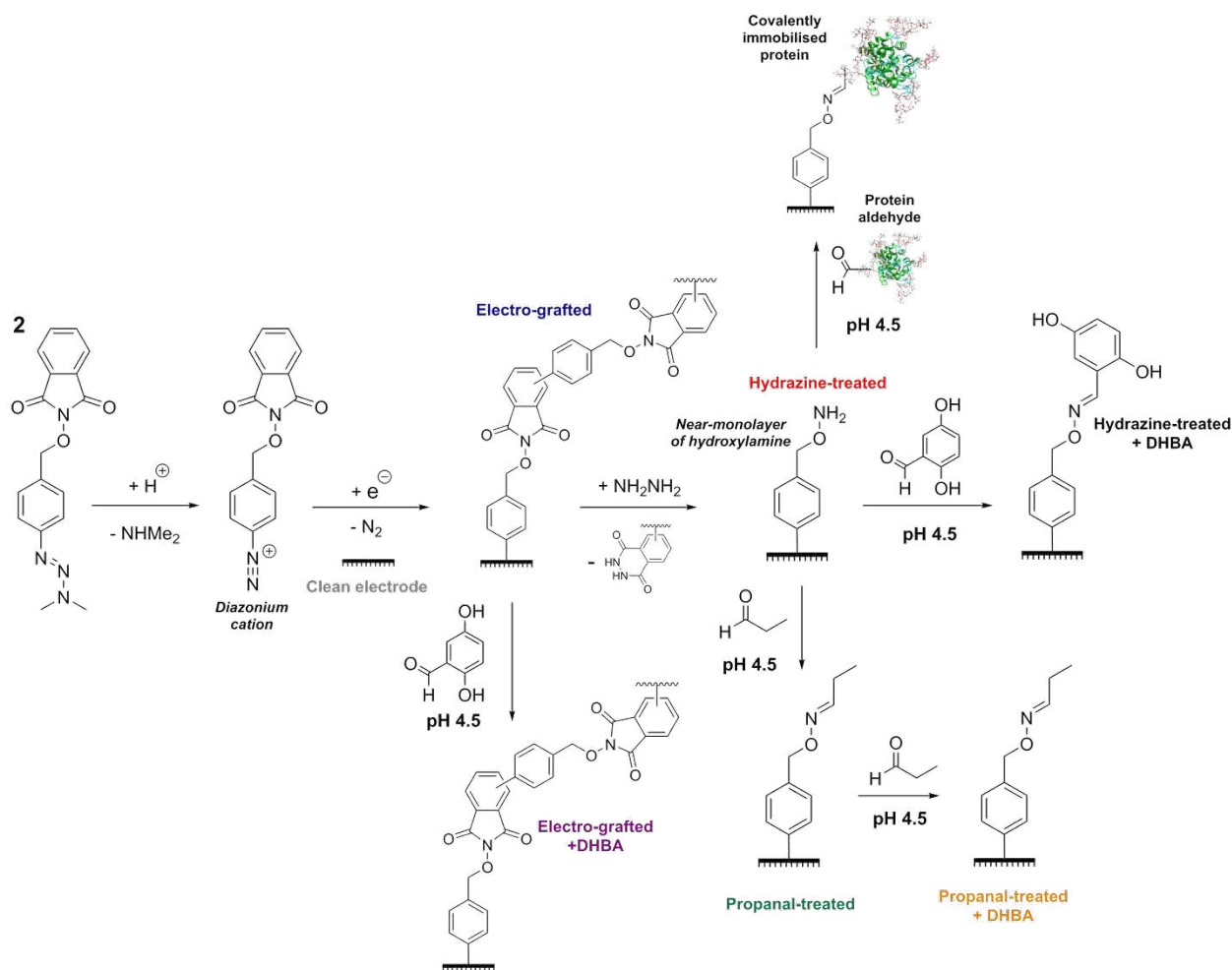
49 **Scheme 2.** The grafting of thick organic multilayers onto electrode surfaces via the reduction of  
50 diazonium cations.  
51  
52  
53  
54  
55  
56  
57  
58  
59  
60



The limitation of the diazonium surface-modification methodology is that multilayer formation often results, as illustrated in Scheme 2.<sup>23-24, 30-31</sup> The nm-scale thickness often associated with such multilayers<sup>32</sup> is too large to support rapid electron transfer to redox active proteins and enzymes anchored onto the surface.<sup>33</sup> Methodologies to achieve a monolayer surface coverages from diazonium electro-grafting have been developed that are based on using sterically hindered aryl diazonium motifs,<sup>34-35</sup> radical scavengers,<sup>36</sup> and the application of short chronoamperometric pulses.<sup>37-38</sup> However, here we utilize a phthalimide-deprotection approach that enables electrochemical functionalization of a variety of surfaces with a near-monolayer of hydroxylamine functionalities, as summarized in Scheme 3. The inspiration for this approach originates from the works of Hauquier<sup>39</sup> and Downard<sup>40</sup> et al, who reported the introduction of amine functionalities onto glassy carbon<sup>39-40</sup> and gold<sup>39</sup> electrodes via the immobilization of a diazonium molecule bearing a  $\pi$ -containing protecting group on the amine moiety.<sup>39-40</sup> The aromatic protecting groups serve as a sacrificial shield that reacts with the excess radicals generated in the diazonium reduction reaction. The subsequent removal of the protecting groups thus strips the electrode of much the thick, inhomogeneous multilayer,<sup>39-40</sup> with Downard using atomic force microscopy (AFM) to prove monolayer formation.<sup>40</sup> This broader concept of protection-deprotection diazonium electro-grafting has also been applied to functionalize surfaces with aldehydes,<sup>41</sup> thiols,<sup>42</sup> and alkynes,<sup>43</sup> although AFM often indicates near-monolayer, rather than strict monolayer, surface modification. We demonstrate that phthalimide-protection/deprotection can be used to yield a near-monolayer

of hydroxylamine-surface functionality. We present the use of a stable triazene precursor which enables generation of diazonium molecules *in situ*<sup>44-46</sup> and makes our methodology amenable to benchtop reaction conditions (Scheme 3). We prove the presence of hydroxylamine groups on the surface using electrochemical and surface analysis techniques.

**Scheme 3.** Summary of the surface modification strategy and aldehyde ligation experiments described in the paper.



We illustrate the broad utility of this new surface-modification methodology by showing the functionalization of glassy carbon, gold and boron doped diamond surfaces, and prove that our hydroxylamine-functionalized surfaces have a high affinity for small molecule aldehydes (Scheme 3). We demonstrate that bioconjugation of an aldehyde-functionalized protein can be performed

1  
2  
3 under biocompatible conditions via the generation of a horseradish peroxidase functionalized gold  
4  
5 electrode.  
6  
7

## 8 9 EXPERIMENTAL SECTION

10  
11 **Synthesis.** The synthesis methodology used to generate (E)-(4-(3,3-dimethyltriaz-1-en-1-  
12 yl)phenyl)methanol, designated **1**, Scheme S1, and (E)-2-((4-(3,3-dimethyltriaz-1-en-1-  
13 yl)benzyl)oxy)isoindoline-1,3-dione, designated **2** and shown in Scheme 3, is described in the SI  
14  
15 where details of all characterisation methods and data (NMR, (ESI)HRMS and FT-IR) is also  
16  
17 presented (Figure S1-S8).  
18  
19  
20  
21  
22  
23

24 **Electrochemical set-up.** Electrochemical experiments were conducted in a water-jacketed all-  
25  
26 glass electrochemical cell capable of supporting a three-electrode setup (constructed in-house). A  
27  
28 thermostated water-circulator (Grant) was used to maintain temperature control. The disk working  
29  
30 electrodes (3 mm diameter) used in the cyclic voltammetry and EIS electrochemical surface-  
31  
32 analysis experiments were either purchased from eDAQ (glassy carbon and gold electrodes) or  
33  
34 Windsor Scientific (boron-doped diamond electrodes). The Pt wire counter electrode was made  
35  
36 in-house from wire of 1 mm diameter purchased from Sigma-Aldrich. The Ag/AgCl/3.0 M sodium  
37  
38 chloride reference electrode was from eDAQ. All potentials have been converted to versus the  
39  
40 standard hydrogen electrode using the correction factor of  $E(\text{V vs SHE}) = E(\text{V vs Ref}) + 0.205$ ,  
41  
42 which was experimentally determined using the ferricyanide redox couple as calibration.<sup>47</sup> The  
43  
44 potentials reported for the experiments performed in 1:5 v:v water:acetonitrile + 0.1 M  
45  
46 tetrabutylammonium hexafluorophosphate ( $\text{Bu}_4\text{NPF}_6$ ) electrolyte do not account for any junction  
47  
48 potential that may exist between the Ag/AgCl/3.0 M sodium chloride reference electrode and the  
49  
50 mixed solvent electrolyte. All experiments that were conducted under a nitrogen atmosphere were  
51  
52  
53  
54  
55  
56  
57  
58  
59  
60

1  
2  
3 carried out in a nitrogen-filled glovebox of dioxygen  $\leq 40$  ppm, otherwise experiments were  
4  
5 performed in air.  
6  
7

8  
9 An EmStat<sup>3</sup> potentiostat (PalmSens) with PSTrace 5.5 for Windows software was used for the  
10  
11 diazonium electro-grafting experiments. The electrochemical assays of surface confined quinone  
12  
13 species were conducted using a CompactStat potentiostat (Ivium technologies) with IviumSoft  
14  
15 software for Windows. The electrochemical impedance spectroscopy experiments were carried out  
16  
17 using a Plamsens4 potentiostat and details of the data analysis are provided in the SI (Figure S9).  
18  
19  
20

21 **Hydroxylamine-functionalization of the disk electrodes.** The disk electrodes were cleaned  
22  
23 using the following procedures. Glassy carbon electrode surfaces were mechanically polished for  
24  
25 1-2 min using 1-5  $\mu\text{m}$  alumina slurry impregnated onto a *WhiteFelt* polishing pad (Buehler).  
26  
27 Electrodes were then rinsed with milliQ water and sonicated in acetonitrile for 5 min. Gold  
28  
29 electrodes were polished for approximately 1 min using nylon polishing pads (Buehler)  
30  
31 impregnated with 1  $\mu\text{m}$  RS PRO Blue Diamond Paste (RS Components Ltd) and then for  
32  
33 approximately 1 min with a 1/10  $\mu\text{m}$  RS PRO Grey Diamond Paste (RS Components Ltd). This  
34  
35 was followed by polishing for approximately 1 min using 1-5  $\mu\text{m}$  alumina slurry impregnated onto  
36  
37 a *WhiteFelt* polishing pad, then rinsing and sonication for 1 min in milliQ water. Electrochemical  
38  
39 polishing was then performed by recording 50 cyclic voltammograms from 0.35 to 1.81 V vs SHE  
40  
41 in 0.5 M  $\text{H}_2\text{SO}_4$  at 100  $\text{mV s}^{-1}$ , after which the electrodes were rinsed with milliQ water and  
42  
43 immersed in in milliQ water until used. Boron doped diamond electrodes were polished for 1-2  
44  
45 min using nylon polishing pads (Buehler) impregnated with 1  $\mu\text{m}$  RS PRO Blue Diamond Paste  
46  
47 (RS Components Ltd) and for approximately 1 min using a 1/10  $\mu\text{m}$  RS PRO Grey Diamond Paste  
48  
49 (RS Components Ltd). The electrodes were then rinsed with milliQ water and sonicated in  
50  
51 acetonitrile for 5 min.  
52  
53  
54  
55  
56  
57  
58  
59  
60

1  
2  
3 Once the disk electrodes were cleaned, they were hydroxylamine-functionalized using the  
4 following procedure for *in situ* diazonium cation generation and electro-grafting, and subsequent  
5 hydrazine deprotection. 2  $\mu\text{L}$  of a 6.6 M hydrochloric acid solution was added to 100  $\mu\text{L}$  of a 15  
6 mM solution of **2** in a 1:5 v:v water:acetonitrile + 0.1 M  $\text{Bu}_4\text{NPF}_6$  solvent system at 0  $^\circ\text{C}$ , triggering  
7 the formation of diazonium cations via protonation of the triazene moiety.<sup>44</sup> 65  $\mu\text{L}$  of this solution  
8 was added to 935  $\mu\text{L}$  of 1:5 v:v water:acetonitrile + 0.1 M  $\text{Bu}_4\text{NPF}_6$  at 0  $^\circ\text{C}$  yielding a solution of  
9 a 1 mM maximum diazonium salt concentration. Electrochemical grafting experiments to yield an  
10 electro-grafted surface (Scheme 3) were carried out by cycling between the potentials shown in  
11 the relevant figures at a scan rate of 20  $\text{mV s}^{-1}$  and 0  $^\circ\text{C}$ . After electrochemical grafting, the  
12 electrode surfaces were cleaned by sonication in acetonitrile for 2 min and then rinsed with milliQ  
13 water before being allowed to dry in air. The hydrazine deprotection step (Scheme 3) was carried  
14 out by adding 155  $\mu\text{L}$  of hydrazine monohydrate to 2 mL ethanol and heating the resultant solution  
15 to 80  $^\circ\text{C}$ . The grafted electrodes were then placed into this solution for either 5 min (glassy carbon  
16 and boron-doped diamond electrodes) or 10 min (gold) with the intention of yielding the  
17 hydroxylamine near-monolayer “hydrazine-treated” surface depicted in Scheme 3. The electrodes  
18 were then allowed to cool for 30 s in a 10  $\mu\text{M}$  ice-cold solution of (aminooxy)acetic acid  
19 hemihydrochloride, a solution designed to prevent cross-contamination of the hydroxylamine  
20 surfaces with trace carbonyl species. Prior to treatment of the surfaces with target aldehyde species  
21 the electrodes were rinsed briefly in ice-cold water and dried under a stream of argon.  
22  
23  
24  
25  
26  
27  
28  
29  
30  
31  
32  
33  
34  
35  
36  
37  
38  
39  
40  
41  
42  
43  
44  
45  
46  
47

48 **Reaction of hydroxylamine-functionalized disk electrodes with aldehyde-containing**  
49 **species.** To investigate propanal binding to hydroxylamine-functionalized glassy carbon surfaces  
50 modified disk electrodes were placed in aqueous pH 4.5 buffer solution (100 mM sodium acetate  
51 + 150 mM sodium chloride) spiked with 5 % v/v propanal for 1 hour at room temperature, after  
52  
53  
54  
55  
56  
57  
58  
59  
60

1  
2  
3 which time the electrodes were rinsed with milliQ water and air-dried before electrochemical  
4 testing, *vide infra*.  
5  
6

7  
8 To investigate 2,5-dihydroxybenzaldehyde binding to hydroxylamine-functionalized glassy  
9 carbon, boron-doped diamond and gold disk electrodes thus-modified disk electrodes were placed  
10 in a 50  $\mu\text{M}$  solution of 2,5-dihydroxybenzaldehyde in aqueous pH 4.5 buffer solution (100 mM  
11 sodium acetate + 150 mM sodium chloride). The reaction was left overnight at room temperature,  
12 after which time the electrodes were rinsed with milliQ water and sonicated with acetonitrile for  
13 30 s prior to cyclic voltammetric interrogation at 25  $^{\circ}\text{C}$  in aqueous pH 4.0 buffer solution (100  
14 mM sodium acetate + 150 mM sodium sulfate).  
15  
16  
17  
18  
19  
20  
21  
22  
23  
24  
25

26 **Oxidized horseradish peroxidase surface-immobilization.** Oxidized horseradish peroxidase  
27 (EZ-Link<sup>TM</sup> Plus Activated Peroxidase) was purchased from Thermo Scientific. For the electrode-  
28 protein ligation experiment, hydroxylamine-functionalized 3 mm gold disk electrodes were treated  
29 with a 50  $\mu\text{M}$  solution of oxidized horseradish peroxidase in aqueous pH 4.5 buffer solution (100  
30 mM sodium acetate + 150 mM sodium chloride). The reaction was left to proceed overnight at  
31 room temperature, after which time the electrodes were rinsed with aqueous pH 7.4 100 mM  
32 sodium phosphate buffer solution prior to electrochemical analysis. Control experiments were  
33 performed by carrying out the same procedure but using non-oxidized, native horseradish  
34 peroxidase (peroxidase from horseradish, Type I, Sigma-Aldrich). The concentration of the  
35 horseradish peroxidase solutions was determined using the extinction coefficient  $\epsilon = 100 \text{ mM cm}^{-1}$   
36 at 403 nm.<sup>48</sup>  
37  
38  
39  
40  
41  
42  
43  
44  
45  
46  
47  
48  
49  
50  
51

52 **Solution-phase analogues of surface chemistry reactions.** As detailed in the SI, solution-  
53 phase experiments were carried out to probe the surface-phase chemistry. Figures S14-25 show  
54  
55  
56  
57  
58  
59  
60

1  
2  
3 the NMR, (ESI)HRMS and FT-IR data of the products isolated from hydrazine deprotection of **2**  
4 to yield (E)-O-(4-(3,3-dimethyltriaz-1-en-1-yl)benzyl)hydroxylamine, designated as **3** (Scheme  
5 S3); oxime reaction of **3** with 2,5-dihydroxybenzaldehyde; and reaction of o-benzylhydroxylamine  
6 with 2,5-dihydroxybenzaldehyde.  
7  
8  
9  
10  
11  
12

13 **X-ray photoelectron spectroscopy.** The X-ray photoelectron spectroscopy (XPS) experiments  
14 were conducted using a monochromated Al K $\alpha$  source at 1486.6 eV (XM1000, Scienta Omicron  
15 GmbH) in an ultrahigh vacuum system with a base pressure below  $2 \times 10^{-10}$  mbar. X-rays were  
16 incident at 22.5° to the sample normal and at 45° to the hemispherical energy analyzer (EA 125,  
17 Scienta Omicron GmbH) used to detect emitted photoelectrons. An input aperture diameter of 6  
18 mm was used for all scans.  
19  
20  
21  
22  
23  
24  
25  
26  
27

28 To prepare the samples for XPS analysis, gold-coated silicon wafer (99.999% (Au), layer  
29 thickness 1000 Å, 99.99% (Ti adhesion layer)) was purchased from Sigma-Aldrich and cut into 8  
30 mm  $\times$  8 mm squares. A solution of acidic piranha (caution: highly corrosive) was prepared by  
31 adding 1 part of 30% hydrogen peroxide to 3 parts of concentrated sulfuric acid. The solution was  
32 used while hot to clean the 8 mm  $\times$  8 mm samples, which were only removed after reaction had  
33 ceased. The gold substrates were then rinsed with water and dried under a stream of argon prior to  
34 electrochemical grafting (Figure S28). Any subsequent hydrazine-treatment was carried out as  
35 described for disk electrodes.  
36  
37  
38  
39  
40  
41  
42  
43  
44  
45  
46

47 Survey scans on the three surfaces tested were measured from a binding energy of 700 eV to 0  
48 eV in -0.3 eV steps and a with dwell time of 0.5 s. To allow comparison of relevant peaks, these  
49 scans were normalized to the average count measured between 600 and 700 eV. High resolution  
50 core level spectra were measured over the range of the O 1s, N 1s and C 1s peaks of interest with  
51  
52  
53  
54  
55  
56  
57  
58  
59  
60

1  
2  
3 -0.05 eV steps and a 1 s dwell time; typically, five separate scans were obtained, then averaged.  
4  
5 For the O 1s and C 1s peaks the data were normalized to the relative weights observed in the survey  
6  
7 spectra. The N 1s data were scaled to give a consistent noise level.  
8  
9

10  
11 **Quartz crystal microbalance with dissipation monitoring.** A Qsense E1 quartz crystal  
12  
13 microbalance with dissipation monitoring (QCM-D) was used to quantify mass changes associated  
14  
15 with the deprotection of the grafted layer and subsequent protein coupling. A QSX301 quartz  
16  
17 crystal microbalance chip purchased from QSense ( $f_0 = (4.95 \pm 0.05)$  MHz) was used as the solid  
18  
19 substrate and cleaned with a solution of basic piranha that was prepared by adding 1 part of 30%  
20  
21 hydrogen peroxide to 3 parts of ammonium hydroxide solution. The resultant solution was then  
22  
23 heated to 60 °C and used for cleaning while hot. Once reaction between the piranha solution and  
24  
25 the gold surface ceased, the gold chip was subjected to UV/ozone treatment prior to  
26  
27 electrochemical grafting. Cyclic voltammograms of the electro-grafting procedure are shown in  
28  
29 Figure S31. Post-grafting, the chip was rinsed in water and then ethanol. After loading into the  
30  
31 QCM-D instrument, the electro-grafted surface was temperature-equilibrated with 50 °C ethanol  
32  
33 in a custom-built open-topped static chamber attached to a standard QSense base. The frequency  
34  
35 and dissipation responses from odd harmonics from 3 to 13 were probed in sequence with a time  
36  
37 resolution of approximately 0.8 s. After thermal equilibrium was reached, hydrazine monohydrate  
38  
39 was added such that an 7 % v/v solution of hydrazine in ethanol was obtained. After deprotection  
40  
41 had been observed via an increase in  $\Delta f$ , the hydrazine ethanol solution was replaced with a  
42  
43 solution of 1  $\mu$ M hydrazine monohydrate in distilled water. This solution was then exchanged with  
44  
45 aqueous pH 4.5 buffer solution (100 mM sodium acetate + 150 mM sodium chloride), then a 35  
46  
47  $\mu$ M solution of horseradish peroxidase in the same buffer was added, and the response in  $\Delta f$   
48  
49 observed. Finally, the solution of horseradish peroxidase was exchanged for ethanol.  
50  
51  
52  
53  
54  
55  
56  
57  
58  
59  
60

## RESULTS AND DISCUSSION

Triazene **1** (Scheme S1 and Figures S1-4) was synthesized from commercially available 4-aminophenol (yield 73%), before derivatization to yield phthalimide-functionalized triazene **2** (yield 51%, Scheme 3 and Figures S5-8). Triazene **2** was designed to permit the functionalization of any conducting surface with a near-monolayer of hydroxylamine. The aryl triazene functional group has been previously used as an acid-labile protecting group for aryl diazonium species,<sup>44-46</sup> and the propensity of **2** to form diazonium species upon protonation is evidenced by the presence of a species of  $m/z$  280.07 in the ESI-MS (Figure S7). The acid-triggered *in situ* generation of the diazonium species from triazene **2** and the subsequent reductive electro-grafting process on a glassy carbon electrode was followed using cyclic voltammetry (Figure 2). The broad reductive wave (negative current) that is observed as the potential of the electrode is decreased from approximately +0.6 to 0 V vs SHE in scan 1 is typical of diazonium reduction,<sup>23-24, 49</sup> and the disappearance of this feature in subsequent scans indicates the formation of a thick multilayer.<sup>39</sup>

50

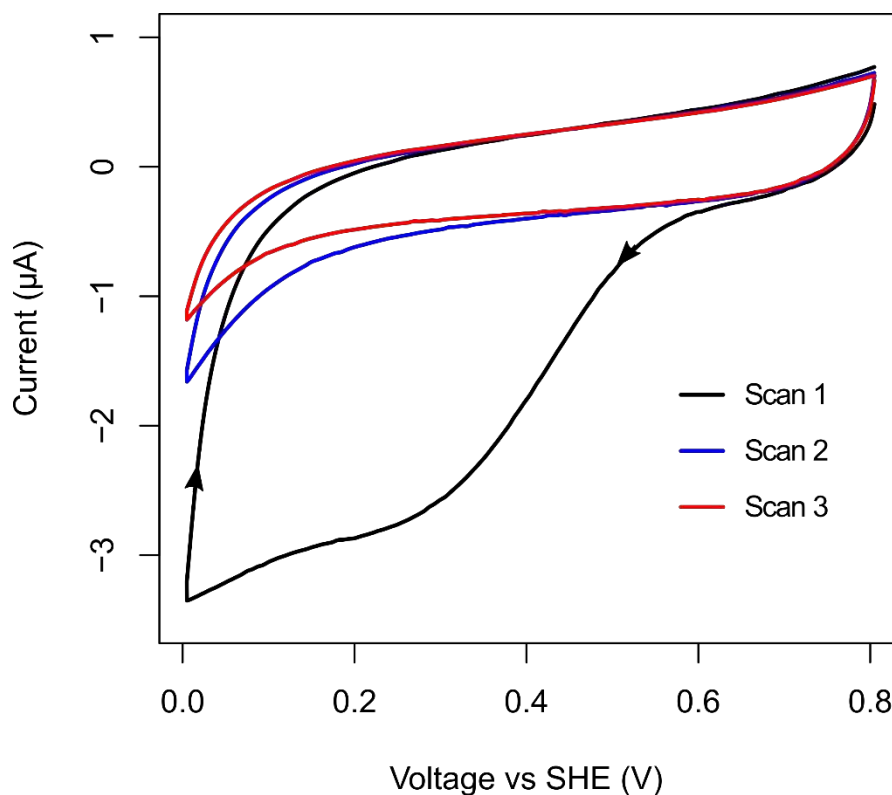


**Figure 2.** Cyclic voltammograms of a glassy carbon electrode during  $20 \text{ mV s}^{-1}$  electroreductive modification scans with the aryl diazonium salt generated *in situ* from **2** in 1:5 v:v water:acetonitrile and  $0.1 \text{ M Bu}_4\text{NPF}_6$ ,  $0 \text{ }^\circ\text{C}$ . The scans commence at the most positive potential, then the voltage is lowered before being increased again. Arrowheads on black scans differentiate between the oxidative and reductive sweeps.

As reported by Hauquier,<sup>39</sup> the treatment of electro-grafted electrode surfaces with a solution of hydrazine monohydrate in ethanol at  $80 \text{ }^\circ\text{C}$  serves to remove phthalimide protecting groups, stripping the multilayer from the electrode surface, see Scheme 3. For our hydroxylamine system, the hydrazine also serves a secondary function, acting as a scavenger for trace carbonyl species

and thus preventing the reaction of the modified surface with contaminant carbonyl compounds such as ethanal or acetone.

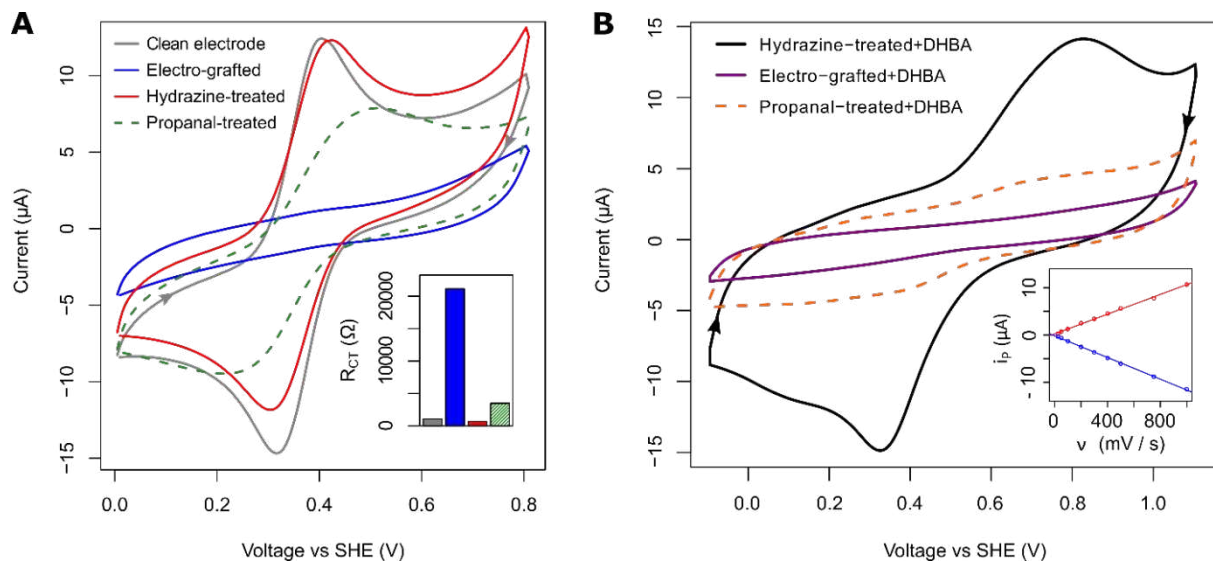


**Figure 3.** (A) Cyclic voltammograms of glassy carbon electrodes from various stages in the modification process and after a “quench” reaction with propanal, all scans were measured at 500  $\text{mV s}^{-1}$  in an aqueous solution of 1 mM ferricyanide and 0.1 M sodium chloride. (A, inset) The change in the resistance to charge transfer ( $R_{CT}$ ) determined from EIS experiments measured on the same electrodes and under the same experimental conditions. (B) Cyclic voltammograms of glassy carbon electrodes from various stages in the modification process and after a “quench” reaction with propanal that have been subsequently reacted with 2,5-dihydroxybenzaldehyde (DHBA). All scans were measured at 500  $\text{mV s}^{-1}$ , nitrogen, in aqueous pH 4.0 buffer solution (100 mM sodium acetate + 150 mM sodium sulfate). (C, inset) Analysis of the quinone-derived baseline-subtracted anodic (red) and cathodic (blue) peak currents shows a linear relationship to scan rate ( $v$ ). In panels A and B the arrowheads differentiate between the oxidative and reductive sweeps.

1  
2  
3  
4  
5  
6  
7 As shown in Figure 3A, the glassy carbon electrode modification process can be monitored via  
8 cyclic voltammetry in aqueous ferricyanide solutions. Unmodified glassy carbon electrodes show  
9 the expected solution-voltammetry responses for reversible ferricyanide electrochemistry,<sup>50</sup> while  
10 electrode surfaces which have been subjected to electro-grafting (Scheme 3) display only a non-  
11 Faradaic (capacitive-only) voltammetric response to the same solution. Glassy carbon electrodes  
12 which have been electro-grafted and subsequently treated with hydrazine show a return to the  
13 typical solution-voltammetry response. The inhibition of the redox chemistry upon electro-grafting  
14 is attributed to the formation of a thick multilayer that is impermeable to the ferricyanide. The fact  
15 that hydrazine-treatment restores the reversible solution voltammetry indicates that deprotection  
16 of the phthalimide moiety strips the impermeable multilayer from the surface of the electrode.  
17  
18  
19  
20  
21  
22  
23  
24  
25  
26  
27  
28  
29

30 Electrochemical impedance spectroscopy (EIS, Figure S9) can also be carried out on different  
31 electrode surfaces in a solution of ferricyanide. As shown in Figure 3A, the changes to the  
32 resistance to charge transfer ( $R_{CT}$ ) values extracted from analysis of this data provide further  
33 evidence that the electro-grafting and hydrazine-treatment processes have a profound effect on the  
34 surface chemistry of a glassy carbon electrode. The high  $R_{CT}$  value of the electro-grafted surface  
35 is consistent with the notion that diazonium-modification forms an electrically insulated multilayer  
36 on the surface of the electrode.  
37  
38  
39  
40  
41  
42  
43  
44  
45  
46

47 Evidence that electro-grafting followed by hydrazine-treatment generates a hydroxylamine  
48 functionalized surface is provided by reacting a thus-modified glassy carbon electrode with  
49 propanal. Propanal is a simple aldehyde which would be expected to undergo facile ligation to a  
50 hydroxylamine-modified surface, generating a neutral oxime species. This can be detected in the  
51  
52  
53  
54  
55  
56  
57  
58  
59  
60

1  
2  
3 EIS measurements in ferricyanide solution, with an increase in  $R_{CT}$  following propanal reaction of  
4 a hydrazine-treated electrode (Figure 3A; Table S1 and Figure S10). Voltammograms measured  
5 in the same ferricyanide solution also highlight that the surface chemistry of the electrode has  
6 changed following reaction with propanal. The drop in peak current and increase in the peak-to-  
7 peak voltage separation is consistent with the generation of a passivated electrode surface.  
8  
9

10  
11  
12 It is possible to estimate the coverage of hydroxylamine functionalities on the hydrazine-treated  
13 electrode surfaces via oxime ligation to the redox active species 2,5-dihydroxybenzaldehyde. This  
14 generates an electrode that shows surface-bound quinone redox chemistry (Figure 3B and Scheme  
15 S2) that is comparable to data in the literature for surface-confined quinones.<sup>51-53</sup> Specifically, the  
16 broad nature of the oxidative peak and the shoulder present in the reductive peak result from the  
17 complicated square scheme that describes the variety of proton-coupled electron-transfer pathways  
18 via which the two-electron quinone redox chemistry can proceed.<sup>53</sup> The large separation in the  
19 potentials of peak oxidative and reductive current is expected based on literature data on surface-  
20 confined quinone species.<sup>51-53</sup> The potential window of the redox process also correlates with  
21 published data<sup>51-53</sup> and solution-phase voltammetry of 2,5-dihydroxybenzaldehyde recorded under  
22 the same conditions as the data in Figure 3 (see Figure S12).  
23  
24  
25  
26  
27  
28  
29  
30  
31  
32  
33  
34  
35  
36  
37  
38  
39  
40  
41

42 The peak-current response scales linearly with scan rate in a manner that is indicative of surface  
43 confinement (Figure 3B and Figure S11).<sup>40, 51-54</sup> The electroactive coverage of the redox active  
44 quinone units, calculated via integration of the baseline-subtracted cathodic peaks,<sup>54</sup> was found to  
45 be 150-170 pmol  $\text{cm}^{-2}$  (Equation S1). This compares well to a theoretical maximum surface  
46 coverage of 182 pmol  $\text{cm}^{-2}$ , calculated by approximating that each electrode-confined quinone-  
47 species is orientated perpendicular to the surface, occupies a circular surface area of  $1.21 \times 10^{-14}$   
48  $\text{cm}^2$  (based on a molecular diameter of 10.27 Å from Chem3D) and is hexagonally close-packed.  
49  
50  
51  
52  
53  
54  
55  
56  
57  
58  
59  
60

1  
2  
3 The experimental coverage data is also in good agreement with the 100-250 pmol cm<sup>-2</sup> coverage  
4 of ferrocene units that has been reported when coupling activated ester ferrocene-derivatives to  
5 glassy carbon electrodes functionalized with monolayers of alkyl amine functionalities.<sup>39</sup>  
6  
7

8  
9  
10  
11 Hydrazine-treated glassy carbon electrodes that have been reacted with propanal prior to  
12 exposure to 2,5-dihydroxybenzaldehyde fail to show surface-bound quinone redox chemistry,  
13 which is consistent with the hydroxylamine electrode-functionalities being unavailable for reaction  
14 with 2,5-dihydroxybenzaldehyde due to quenching via oxime ligation to propanal (Figure 3B).  
15  
16 The reaction of hydrazine-treated electrodes with hydroquinone, rather than the aldehyde  
17 containing derivative 2,5-dihydroxybenzaldehyde, also fails to yield surface-confined quinone  
18 species (Figure S13). This shows that the presence of the aldehyde on 2,5-dihydroxybenzaldehyde  
19 is critical to the surface confinement of a quinone-containing molecule, and that surface-confined  
20 redox chemistry is not observed due to simple adsorption. The proclivity of 2,5-  
21 dihydroxybenzaldehyde towards oxime ligation with solution-phase hydroxylamine species has  
22 also been demonstrated (Scheme S3, Figures S14-S25).  
23  
24  
25  
26  
27  
28  
29  
30  
31  
32  
33  
34  
35  
36

37 To demonstrate that the hydroxylamine-surface functionalization methodology can be applied  
38 to a wide range of different conducting materials, boron-doped diamond and gold electrodes were  
39 modified using the same two-step diazonium electroreduction and subsequent deprotection  
40 strategy previously described for glassy carbon. As with glassy carbon, the diazonium electro-  
41 grafting process was monitored by cyclic voltammetry, see Figure 4. It is notable that both the  
42 onset potential and current changes with electrode material, an observation which is consistent  
43 with diazonium electrografting studies by other authors.<sup>55-58</sup> For both boron-doped diamond and  
44 gold, the substantial drop in reductive current which follows the first scan is again interpreted as  
45 evidence that a multilayer has formed on the electrode surface.  
46  
47  
48  
49  
50  
51  
52  
53  
54  
55  
56  
57  
58  
59  
60

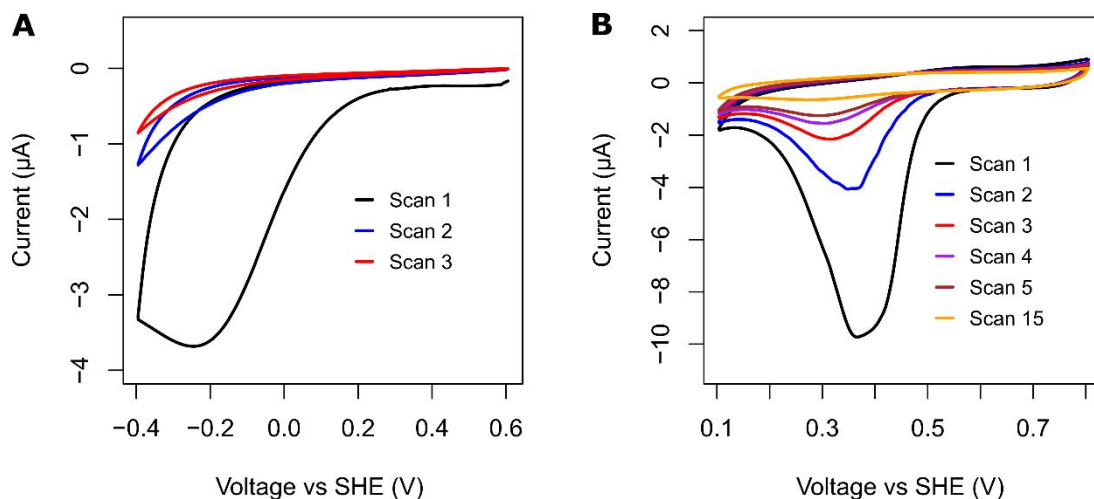


**Figure 4.** Cyclic voltammograms of (A) boron doped diamond and (B) gold electrodes during 20  $\text{mV s}^{-1}$  electroreductive modification scans with the aryl diazonium salt generated *in situ* from **2** in 1:5 v:v water:acetonitrile and 0.1 M  $\text{Bu}_4\text{NPF}_6$ , 0  $^\circ\text{C}$ . The scans commence at the most positive potential, then the voltage is lowered to the most reductive potential before being increased again.

The reactivity of the boron-doped diamond and gold electrode surface-hydroxylamine groups with aldehyde species in solution is again probed using 2,5-dihydroxybenzaldehyde. Post-reaction, the presence of oxime-linked quinone-electrode species is detected in the cyclic voltammograms shown in Figure 5. As in the analogous glassy carbon experiments (Figure 3), the intensity of the peak current of the baseline-subtracted gold and boron doped diamond redox signals scales linearly with scan rate, as expected for a surface-confined quinone species (Figure 5, Figure S11).<sup>40, 52, 54</sup>

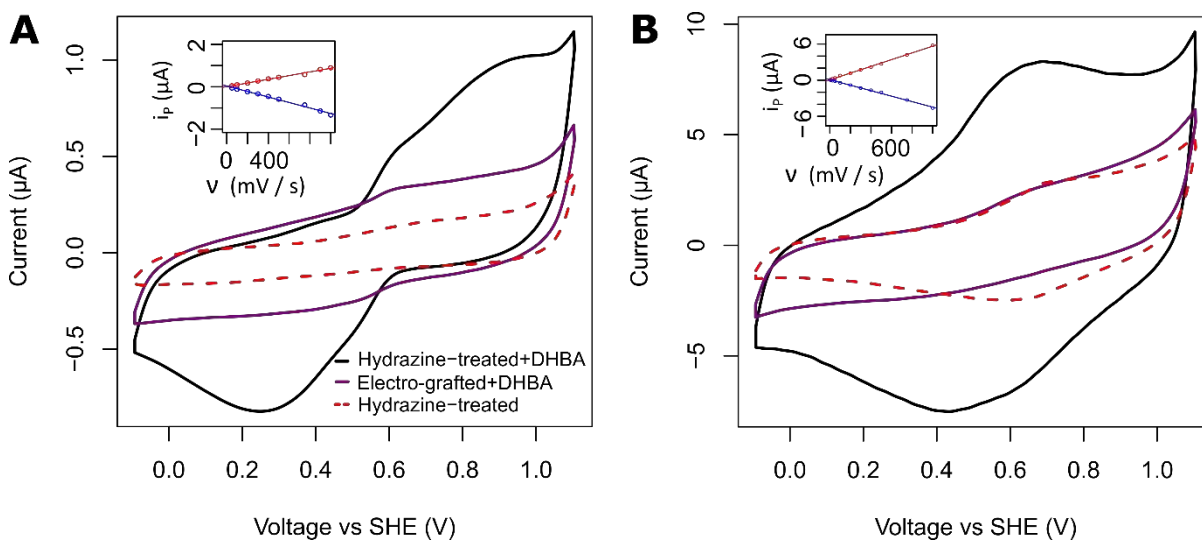


**Figure 5.** Cyclic voltammetry of (A) boron doped diamond electrode and (B) gold electrode which have been electro-grafted with compound **2**, and then (black line) hydrazine-treated prior to reaction with 2,5-dihydroxybenzaldehyde (DHBA), or (purple line) treated with DHBA while still in the electro-grafted state. (Red dashed line) Data from a control experiment where the hydrazine-treatment is not followed by DHBA reaction. (Insets) The magnitude of the baseline-subtracted (red) anodic and (blue) cathodic peak currents ( $i_p$ ) vs scan rate ( $v$ ). The voltammograms shown were recorded at 500 mV s<sup>-1</sup>, 25 °C, nitrogen, in an aqueous pH 4.0 buffer solution (100 mM sodium acetate + 150 mM sodium sulfate).

On the gold electrodes, a quinone surface-coverage of approximately 100 pmol cm<sup>-2</sup> is derived. This value can be compared to the glassy carbon value of surface-coverage of approximately 160 pmol cm<sup>-2</sup>. According to the literature, achieving a lower surface density modification on a gold electrode relative to glassy carbon is to be expected, with previous studies indicating that the coverage of ferrocene units which could be coupled to a gold surface functionalized with a

1  
2  
3 monolayer of alkyl amine functionalities was 5 to 12.5 times lower than that achieved using  
4  
5 similarly functionalized glassy carbon electrodes.<sup>39</sup>  
6  
7

8  
9 The surface modification of a gold electrode was further probed by using atomic force  
10  
11 microscopy (AFM) to compare the surface morphology of gold that has been electro-grafted,  
12  
13 hydrazine-treated and subsequently reacted with propanal with a gold surface control that was not  
14  
15 diazonium-electrografted. As shown in Figure S26, the AFM imaging is consistent with the  
16  
17 formation of a monolayer or a near-monolayer rather than a multilayer. Taking the electrochemical  
18  
19 coverage data in context with the quinone coverage, we therefore conclude that the protection-  
20  
21 deprotection methodology described yields glassy carbon and gold surfaces modified with a near-  
22  
23 monolayer coverage of hydroxylamines.  
24  
25  
26  
27

28  
29 Integration of the peak area of baseline-subtracted quinone signals quantifies the surface  
30  
31 coverage of hydroxylamine moieties on boron doped diamond electrodes as approximately 40  
32  
33 pmol cm<sup>-2</sup>. This value is reproducible in repeat experiments using different electrodes. This is a  
34  
35 lower coverage than reported for ferrocene-coated boron-doped diamond electrodes generated via  
36  
37 either Cu<sup>I</sup>-catalysed click reaction between diazonium electro-grafted phenyl azide and  
38  
39 ethynylferrocene (250 pmol cm<sup>-2</sup>);<sup>59</sup> or photochemical immobilization of vinylferrocene (450 pmol  
40  
41 cm<sup>-2</sup>).<sup>60</sup> Although these published modification strategies do not aim for struct monolayer  
42  
43 coverage, and may therefore establish upper limit coverage ranges for boron doped diamond, it is  
44  
45 notable that the quinone oxime-ligation coverage we measure on boron doped diamond is also far  
46  
47 lower than the analogous glassy carbon measurement, a fact that is incongruent to the similarities  
48  
49 in the electrografting voltammetry. Further experiments were therefore conducted to probe the  
50  
51 impact of the hydrazine deprotection step on the surface chemistry of electro-grafted boron-doped  
52  
53 diamond electrodes, using EIS and cyclic voltammetry measurements of Fe(CN)<sub>6</sub><sup>3-/4-</sup> in solution  
54  
55  
56  
57  
58  
59  
60

1  
2  
3 (Table S1, Figure S10, Figure S27). Although the data is again consistent with the conclusion that  
4  
5 hydrazine-treatment again strips a multilayer that results from the electro-grafting process, the  
6  
7 drop in  $R_{CT}$  (6226 to 444.1  $\Omega$ ) and changes in solution voltammetry are subtler than on glassy  
8  
9 carbon. We therefore speculate that both a physisorbed and electro-grafted layer is deposited at  
10  
11 BDD, and the physisorbed groups are largely removed during cleaning. Improving the density of  
12  
13 coverage on boron doped diamond will therefore need to be a key aim of future work.  
14  
15  
16  
17

18 The ability to modify gold, a metallic substrate, provides the opportunity to probe the  
19  
20 derivatization state of the electrode surface via X-ray photoelectron spectroscopy (XPS). The  
21  
22 standard voltammetric methodology for electro-grafting **2** onto surfaces was applied to two gold-  
23  
24 coated silicon wafers that had been cleaned using acidic piranha solution (Figure S28), and one of  
25  
26 these surfaces was subsequently hydrazine-treated. XPS measurements were then made of the two  
27  
28 modified gold surfaces and a control, non-functionalized, piranha-cleaned gold surface. Evidence  
29  
30 for multilayer formation on the electro-grafted surface is indicated by comparing the survey spectra  
31  
32 data for this surface relative to that for the control clean unmodified gold surface; the carbon-to-  
33  
34 gold and oxygen-to-gold peak ratios both increase for the modified surface relative to those for  
35  
36 clean gold (Figure 6A).  
37  
38  
39  
40  
41  
42  
43  
44  
45  
46  
47  
48  
49  
50  
51  
52  
53  
54  
55  
56  
57  
58  
59  
60

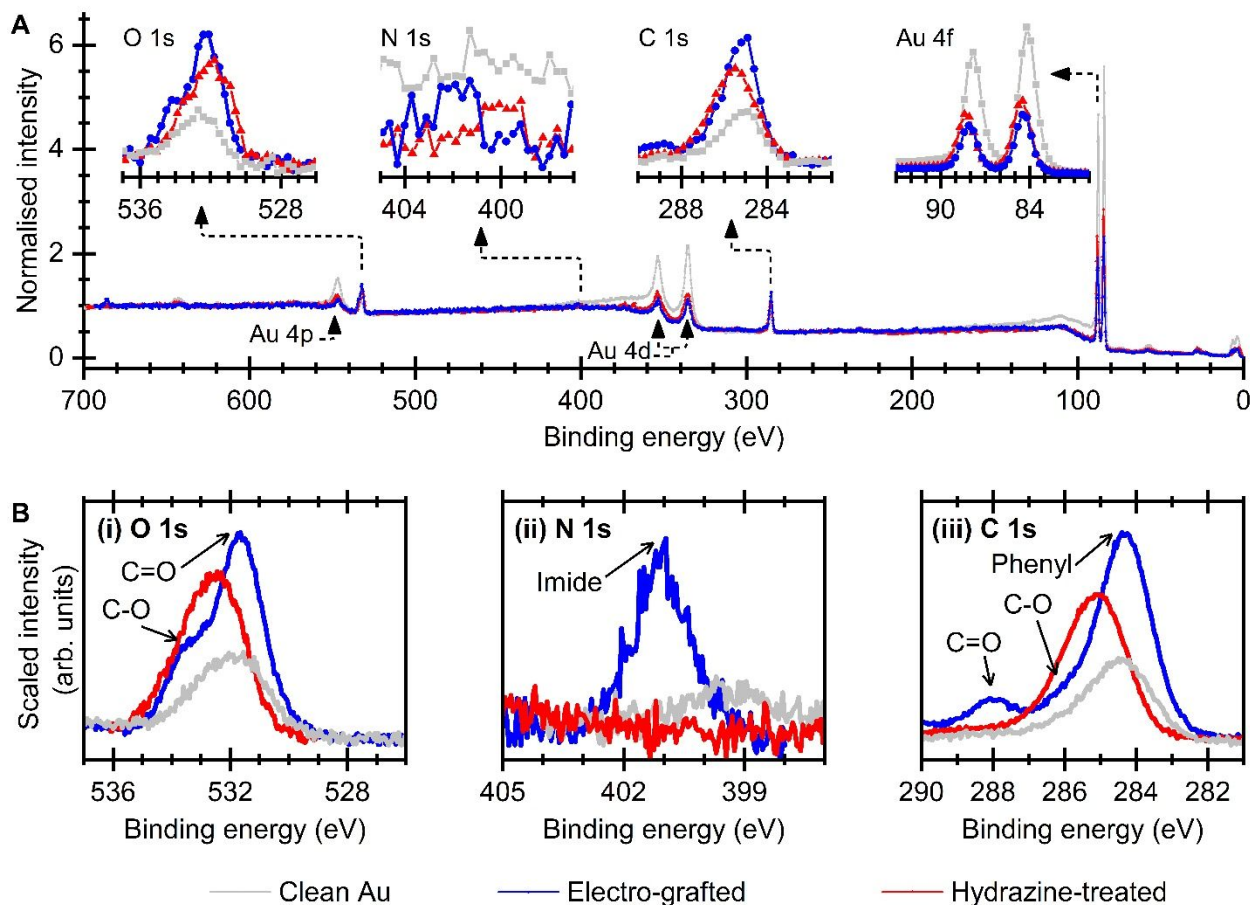


**Figure 6.** XPS of the surface of a gold-coated silicon wafer at different states of functionalization. (A) Survey scans, each with the intensity normalized to the average count between 600 and 700 eV. (B) Higher resolution scans of O 1s, N 1s and C 1s peaks. For (i) and (iii) the relative intensities were scaled using the survey scan data while for (ii) data is scaled to the noise level.

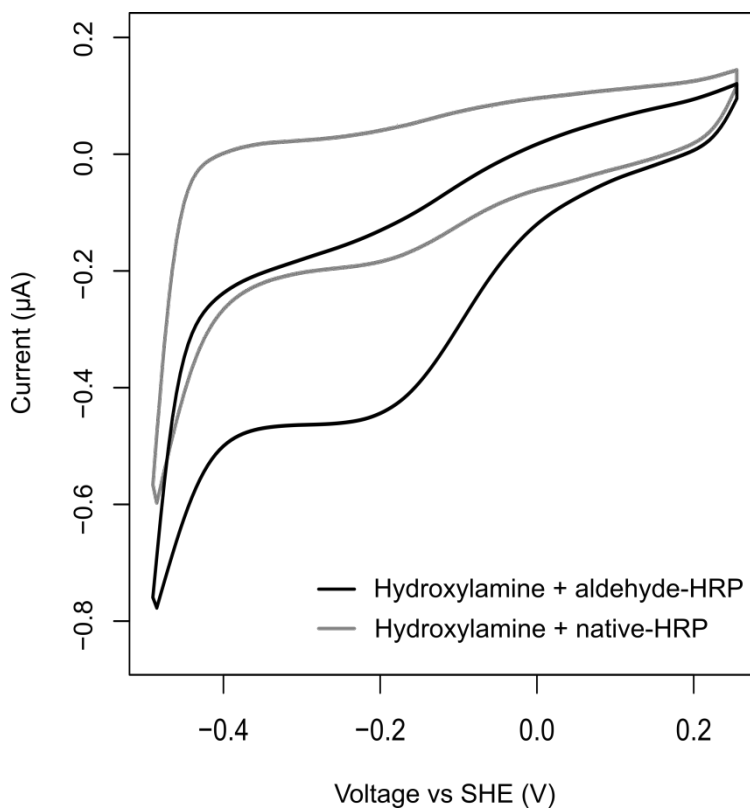
In detailed scans, the peak positions attributed to the different carbon and oxygen environments on the electro-grafted surface are expected based on the molecular structure of **2**,<sup>61</sup> with phenyl (~284.5 eV), C-O (~286.5 eV), and C=O (~288 eV) bonding features present in the C 1s spectra and C-O (531.5 eV) and C=O (533 eV) features in the O 1s spectra. The energy of the nitrogen

1  
2  
3 peak at ~401 eV is also consistent with that observed for imide-type nitrogen atoms (Figure 6B).<sup>62</sup>  
4  
5 Thus, the XPS data supports the structure of the electro-grafting surface shown in Scheme 3. The  
6  
7 notion that hydrazine deprotection of the phthalimide group strips a multilayer off electro-grafted  
8  
9 gold surfaces is evidenced by the drop in the normalized intensity of the survey scan carbon and  
10  
11 oxygen peaks following hydrazine-treatment, and loss of the phenyl signal (Figure 6A).  
12  
13  
14

15  
16 Horseradish peroxidase (HRP) is a highly glycosylated enzyme,<sup>16-18</sup> the glycans of which display  
17  
18 many cis 1,2-diol sites that are converted into aldehydes via periodate oxidation (Figure 1A).<sup>16-18</sup>  
19  
20 Gold electrodes in the hydrazine-treated, hydroxylamine-functionalized modification state were  
21  
22 reacted with either oxidized (aldehyde-containing) horseradish peroxidase or native (aldehyde-  
23  
24 free) horseradish peroxidase. We conclude that the aldehyde-containing horseradish peroxidase is  
25  
26 ligated to the modified electrode via oxime bond formation because subsequent cyclic  
27  
28 voltammetry (25 °C, nitrogen, pH 7.4) shows an intense reductive peak centered at approximately  
29  
30 -0.15 V vs SHE and a broad oxidative peak centered around 0 V vs SHE (black line, Figure 7).  
31  
32 The position of this signal correlates with that reported for other examples of immobilized  
33  
34 horseradish peroxidase participating in direct-electron transfer with an underlying electrode  
35  
36 surface and is attributed to the Fe<sup>2+/3+</sup> redox couple of the heme.<sup>8-9</sup>  
37  
38  
39  
40

41  
42 Experiments using native horseradish peroxidase show that the faradaic current originating from  
43  
44 heme redox chemistry is approximately 4-fold smaller for a hydroxylamine-coated gold electrode  
45  
46 reacted with the aldehyde-free native horseradish peroxidase (grey line, Figure 7). This is  
47  
48 consistent with the native enzyme being unable to partake in oxime ligation to the electrode  
49  
50 surface, resulting in poorer electroactive coverage. Additional control experiments (Figure S29)  
51  
52 further confirm our assignment of the faradaic signals to the redox activity of competent  
53  
54 horseradish peroxidase immobilized on the electrode; this current is greatly diminished when  
55  
56  
57  
58  
59  
60

1  
2  
3 either boiled aldehyde-containing enzyme (i.e. natured protein and free heme) is applied to a  
4 hydrazine-treated electrode, or native (aldehyde-free) horseradish peroxidase is applied to bare  
5 gold, or when a hydrazine-treated electrode surface is incubated with an enzyme-free buffer  
6 solution, or when a hydrazine-treated electrode surface is incubated with an enzyme-free buffer  
7 solution (Figure S29).  
8  
9  
10  
11  
12



40  
41  
42  
43  
44  
45  
46  
47  
48  
49  
50  
51  
52  
53  
54  
55  
56  
57  
58  
59  
60

**Figure 7.** 30 mV s<sup>-1</sup> cyclic voltammograms from when the oxidized, aldehyde-containing enzyme is reacted with a hydrazine-treated gold electrode (black line), and hydrazine-treated electrode surfaces are reacted with native (aldehyde-free) horseradish peroxidase (gray line). All experiments were conducted under nitrogen at 25 °C in pH 7.4 100 mM sodium phosphate buffer solution.

1  
2  
3 Enzyme-free experiments using hydrazine-treated, hydroxylamine-functionalized gold  
4 electrodes showed that these surfaces are highly effective at catalyzing the electroreduction of  
5  $\text{H}_2\text{O}_2$  (Figure S30). This precluded the chronoamperometric detection of the enzymatic activity of  
6 immobilized horseradish peroxidase. Further evidence for the immobilization of aldehyde-  
7 containing horseradish peroxidase onto hydrazine-treated gold electrode surfaces was instead  
8 obtained via quartz crystal microbalance with dissipation monitoring (QCM-D).  
9

10  
11 A gold-coated quartz crystal microbalance (QCM) sensor was electrochemically grafted with **2**  
12 (Figure S31) and washed successively in water and ethanol to remove any non-covalently attached  
13 organic material. This substrate was then temperature-equilibrated with 50 °C ethanol in the  
14 QCM-D apparatus and data logging commenced after thermal equilibrium was reached (Figure 8).  
15  
16 The experimental temperature may induce protein denaturation, but such conditions are required  
17 for the deprotective hydrazine-treatment step and to ensure that oxime ligation occurs over a  
18 timescale shorter than response drift from the QCM-D.  
19  
20  
21  
22  
23  
24  
25  
26  
27  
28  
29  
30  
31  
32

33 Upon the addition of hydrazine monohydrate (▼, Figure 8) the QCM-D showed an immediate  
34 decrease in  $\Delta f$  and a concomitant rise in  $\Delta d$  that is attributable to the change in solution viscosity.<sup>63</sup>  
35 The subsequent gradual increase in  $\Delta f$  is evidence of a decrease in the mass on the surface of the  
36 chip; this is attributed to hydrazine-deprotection of the phthalimide stripping multilayers from the  
37 electrode surface (Scheme 3).<sup>63-64</sup> The dissipation value,  $d$ , is strongly influenced by not only the  
38 viscoelasticity of the adlayer but also by the density and viscosity of the bulk fluid above the film,<sup>65</sup>  
39 which complicates analysis of this region of the trace.  
40  
41  
42  
43  
44  
45  
46  
47  
48

49 At approximately 18.5 min, the hydrazine ethanol solution was replaced with a 1  $\mu\text{M}$  hydrazine  
50 aqueous solution, and at approximately 23.5 min this solution was exchanged with pH 4.5 buffer  
51 (Figure 8). Due to concerns regarding reaction of the hydrazine-treated surface with trace  
52  
53  
54  
55  
56  
57  
58  
59  
60

contaminant aldehyde and ketone species, a 35  $\mu\text{M}$  solution of horseradish peroxidase was added at approximately 25 min ( $\nabla$ , Figure 8), which was before full thermal equilibrium was reached. Enzyme ligation to the surface can be inferred from the steady drop in  $\Delta f$  between 28 and 40 min (Figure 8, inset), which is indicative of an increased adsorbed mass on the QCM sensor;<sup>64, 66</sup> the concomitant increases in  $\Delta d$ , is also attributed to formation of a protein film.<sup>64, 66</sup> Using the equation  $\Delta m = C\Delta f$ , where  $C = -17.8 \text{ ng cm}^{-2} \text{ Hz}^{-1}$  for this system,<sup>63</sup> we estimate the mass change,  $\Delta m$ , to be  $2 \mu\text{g cm}^{-2}$  during protein ligation; this equates to a coverage of  $50 \text{ pmol cm}^{-2}$ .

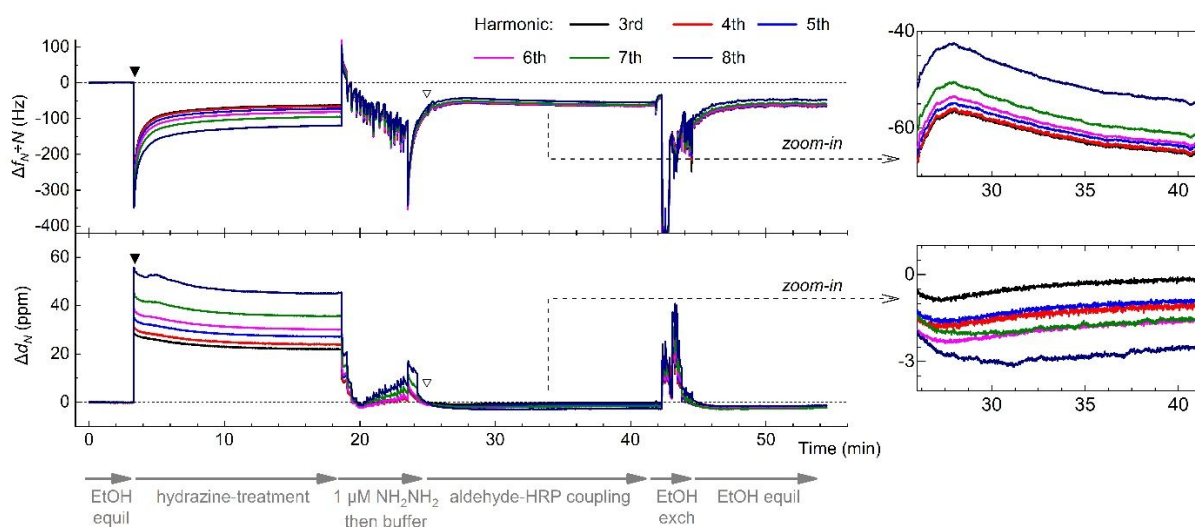


**Figure 8.** QCM-D results of frequency change ( $\Delta f$ ) and dissipation change ( $\Delta d$ ) against time for a gold-coated quartz crystal microbalance sensor electro-grafted with 2 prior to the start of the experiment. Subsequent treatments are as indicated above the plot. The experiment was conducted at 50  $^{\circ}\text{C}$ . Values for  $\Delta f$  are divided by the harmonic number (Q-sense convention).

## SUMMARY AND CONCLUSIONS

The concept of generating a monolayer of amine functionalities on a surface via the electroreduction and subsequent deprotection of protected-amine containing diazonium salts has inspired us to harness protecting group chemistry to generate surfaces modified with a near-

1  
2  
3 monolayer of hydroxylamine. We demonstrate the utility of such surfaces for immobilizing  
4  
5 aldehyde-containing molecules by making electrochemical measurements on surface-immobilized  
6  
7 hydroquinone and horseradish peroxidase, with immobilization of target aldehyde species being  
8  
9 achieved at dilute aldehyde concentrations (50  $\mu\text{M}$ ) and mild pH. We hope that this methodology  
10  
11 will find a broad range of applications. The ability to functionalize semi-conducting and  
12  
13 conducting substrates with hydroxylamine near-monolayers should be useful in stabilizing small  
14  
15 molecule catalysts in photochemistry and solar fuel applications.<sup>67</sup> The immobilization of  
16  
17 glycosylated enzymes, such as HRP, onto solid scaffolds can be utilized in the development of  
18  
19 continuous flow biocatalysts reactors;<sup>7</sup> and hydroxylamine-decorated nanoparticles have already  
20  
21 shown promise as drug delivery vehicles.<sup>68</sup> It is of note that although they were not required here,  
22  
23 simple organic molecules have been identified that act as oxime reaction catalysts, speeding up the  
24  
25 rate of reaction and permitting protein aldehyde-to-hydroxylamine ligation at neutral pH.<sup>69</sup> Thus,  
26  
27 the presented methodology can be developed for immobilizing proteins or enzymes which are less  
28  
29 robust than horseradish peroxidase.  
30  
31  
32  
33  
34  
35

## 36 ASSOCIATED CONTENT

### 39 **Supporting Information.**

40  
41  
42  
43 Synthesis methodology; buffer solution preparation; electrochemical impedance spectroscopy  
44  
45 methods and results; 2,5-dihydroxybenzaldehyde surface coverage experiments and analysis  
46  
47 methodology; quinone control experiments; solution ligation experiments and product analysis;  
48  
49 atomic force microscopy on gold; solution ferricyanide voltammetry at modified boron-doped  
50  
51 diamond electrodes; electro-grafting of gold surfaces for XPS; control electrochemical  
52  
53  
54  
55  
56  
57  
58  
59  
60

1  
2  
3 horseradish peroxidase experiments; electro-grafting for QCM-D; RScript code for cyclic  
4  
5 voltammetry analysis.  
6  
7

## 8 AUTHOR INFORMATION

### 11 **Corresponding Author**

12  
13  
14 \*E-mail martin.fascione@york.ac.uk, alison.parkin@york.ac.uk.  
15  
16

### 17 **Author Contributions**

18  
19  
20 All synthesis, characterization and cyclic voltammetry experiments were designed by AParkin,  
21  
22 MAF and NDY and conducted by NDY with assistance from JD-F. EIS data was collected and  
23  
24 analyzed by MRD. QCM-D experiments were conducted and analyzed by CFB with assistance  
25  
26 from NDY. XPS experiments were conducted by PB with assistance from NDY and data was  
27  
28 analyzed by AParkin with assistance from Apratt and PB. The manuscript was written through  
29  
30 contributions of all authors. All authors have given approval to the final version of the  
31  
32 manuscript.  
33  
34  
35  
36

## 37 ACKNOWLEDGMENTS

38  
39 Abigail Mortimer (UoY) is thanked for skillful construction of the electrochemical glassware. Dr  
40  
41 S P Tear (UoY) is thanked for help in making the AFM measurements. Prof. Gideon Davies  
42  
43 (UoY) is also gratefully acknowledged for valuable scientific discussions. This work was  
44  
45 supported by the Biotechnology and Biological Sciences Research Council (BBSRC, studentship  
46  
47 BB/M011151/1 to NDJY).  
48  
49  
50

## 51 REFERENCES

- 52  
53  
54 1. Spicer, C. D.; Davis, B. G., Selective chemical protein modification. *Nat. Commun.* **2014**,  
55 5, 4740.  
56  
57  
58  
59  
60

2. Boutureira, O.; Bernardes, G. J. L., Advances in Chemical Protein Modification. *Chem. Rev.* **2015**, *115* (5), 2174-2195.
3. Zhang, Y.; Park, K.-Y.; Suazo, K. F.; Distefano, M. D., Recent progress in enzymatic protein labelling techniques and their applications. *Chem. Soc. Rev.* **2018**, *47* (24), 9106-9136.
4. Meldal, M.; Schoffelen, S., Recent advances in covalent, site-specific protein immobilization. *F1000Res.* **2016**, *5* (2303).
5. Yates, N. D. J.; Fascione, M. A.; Parkin, A., Methodologies for “Wiring” Redox Proteins/Enzymes to Electrode Surfaces. *Chem. - Eur. J.* **2018**, *24* (47), 12164-12182.
6. Algar, W. R.; Dawson, P.; Medintz, I. L., *Chemoselective and Bioorthogonal Ligation Reactions: Concepts and Applications*. Wiley: 2017.
7. Britton, J.; Majumdar, S.; Weiss, G. A., Continuous flow biocatalysis. *Chem. Soc. Rev.* **2018**, *47* (15), 5891-5918.
8. Nicolini, J. V.; Ferraz, H. C.; de Resende, N. S., Immobilization of horseradish peroxidase on titanate nanowires for biosensing application. *J. Appl. Electrochem.* **2016**, *46* (1), 17-25.
9. Polsky, R.; Harper, J. C.; Dirk, S. M.; Arango, D. C.; Wheeler, D. R.; Brozik, S. M., Diazonium-Functionalized Horseradish Peroxidase Immobilized via Addressable Electrodeposition: Direct Electron Transfer and Electrochemical Detection. *Langmuir* **2007**, *23* (2), 364-366.
10. Agten, S. M.; Dawson, P. E.; Hackeng, T. M., Oxime conjugation in protein chemistry: from carbonyl incorporation to nucleophilic catalysis. *J. Pept. Sci.* **2016**, *22* (5), 271-279.
11. Arslan, M.; Tasdelen, M. A., Click Chemistry in Macromolecular Design: Complex Architectures from Functional Polymers. *Chemistry Africa* **2019**, *2* (2), 195-214.
12. Appel, M. J.; Bertozzi, C. R., Formylglycine, a post-translationally generated residue with unique catalytic capabilities and biotechnology applications. *ACS Chem. Biol.* **2015**, *10* (1), 72-84.
13. Brabham, R. L.; Spears, R. J.; Walton, J.; Tyagi, S.; Lemke, E. A.; Fascione, M. A., Palladium-unleashed proteins: gentle aldehyde decaging for site-selective protein modification. *Chem. Comm.* **2018**, *54* (12), 1501-1504.
14. Spears, R. J.; Fascione, M. A., Site-selective incorporation and ligation of protein aldehydes. *Org. Biomol. Chem.* **2016**, *14* (32), 7622-7638.
15. Ali, A. A.; Hasan, M. A.; Zaki, M. I., Dawsonite-Type Precursors for Catalytic Al, Cr, and Fe Oxides: Synthesis and Characterization. *Chemistry of Materials* **2005**, *17* (26), 6797-6804.
16. Wisdom, G. B., Horseradish Peroxidase Labeling of Antibody Using Periodate Oxidation. In *The Protein Protocols Handbook*, Walker, J. M., Ed. Humana Press: Totowa, NJ, 1996; pp 273-274.
17. Baker, M. R.; Tabb, D. L.; Ching, T.; Zimmerman, L. J.; Sakharov, I. Y.; Li, Q. X., Site-Specific N-Glycosylation Characterization of Windmill Palm Tree Peroxidase Using Novel Tools for Analysis of Plant Glycopeptide Mass Spectrometry Data. *J. Proteome Res.* **2016**, *15* (6), 2026-2038.
18. Capone, S.; Pletzenauer, R.; Maresch, D.; Metzger, K.; Altmann, F.; Herwig, C.; Spadiut, O., Glyco-variant library of the versatile enzyme horseradish peroxidase. *Glycobiology* **2014**, *24* (9), 852-863.
19. Brabham, R.; Fascione, M. A., Pyrrolysine Amber Stop-Codon Suppression: Development and Applications. *ChemBioChem* **2017**, *18* (20), 1973-1983.

- 1  
2  
3 20. Christman, K. L.; Broyer, R. M.; Tolstyka, Z. P.; Maynard, H. D., Site-specific protein  
4 immobilization through N-terminal oxime linkages. *J. Mater. Chem.* **2007**, *17* (19), 2021-2021.
- 5 21. Park, S.; Yousaf, M. N., An Interfacial Oxime Reaction To Immobilize Ligands and Cells  
6 in Patterns and Gradients to Photoactive Surfaces. *Langmuir* **2008**, *24* (12), 6201-6207.
- 7 22. Gooding, J. J.; Ciampi, S., The molecular level modification of surfaces: from self-  
8 assembled monolayers to complex molecular assemblies. *Chem. Soc. Rev.* **2011**, *40* (5), 2704-  
9 2718.
- 10 23. Mahouche-Chergui, S.; Gam-Derouich, S.; Mangeney, C.; Chehimi, M. M., Aryl  
11 diazonium salts: a new class of coupling agents for bonding polymers, biomacromolecules and  
12 nanoparticles to surfaces. *Chem. Soc. Rev.* **2011**, *40* (7), 4143-4166.
- 13 24. Chehimi, M. M., *Aryl Diazonium Salts: New Coupling Agents in Polymer and Surface*  
14 *Science*. Wiley-VCH Verlag GmbH & Co: 2012.
- 15 25. Wang, J.; Carlisle, J. A., Covalent immobilization of glucose oxidase on conducting  
16 ultrananocrystalline diamond thin films. *Diam. Relat. Mater.* **2006**, *15* (2), 279-284.
- 17 26. Zhang, X.; Tretjakov, A.; Hovestaedt, M.; Sun, G.; Syritski, V.; Reut, J.; Volkmer, R.;  
18 Hinrichs, K.; Rappich, J., Electrochemical functionalization of gold and silicon surfaces by a  
19 maleimide group as a biosensor for immunological application. *Acta Biomater.* **2013**, *9* (3),  
20 5838-5844.
- 21 27. Gam-Derouich, S.; Lamouri, A.; Redeuilh, C.; Decorse, P.; Maurel, F.; Carbonnier, B.;  
22 Beyazit, S.; Yilmaz, G.; Yagci, Y.; Chehimi, M. M., Diazonium Salt-Derived 4-  
23 (Dimethylamino)phenyl Groups as Hydrogen Donors in Surface-Confined Radical  
24 Photopolymerization for Bioactive Poly(2-hydroxyethyl methacrylate) Grafts. *Langmuir* **2012**,  
25 *28* (21), 8035-8045.
- 26 28. Salmi, Z.; Lamouri, A.; Decorse, P.; Jouini, M.; Boussadi, A.; Achard, J.; Gicquel, A.;  
27 Mahouche-Chergui, S.; Carbonnier, B.; Chehimi, M. M., Grafting polymer-protein bioconjugate  
28 to boron-doped diamond using aryl diazonium coupling agents. *Diam. Relat. Mater.* **2013**, *40*,  
29 60-68.
- 30 29. Uetsuka, H.; Shin, D.; Tokuda, N.; Saeki, K.; Nebel, C. E., Electrochemical Grafting of  
31 Boron-Doped Single-Crystalline Chemical Vapor Deposition Diamond with Nitrophenyl  
32 Molecules. *Langmuir* **2007**, *23* (6), 3466-3472.
- 33 30. Juan-Colás, J.; Parkin, A.; Dunn, K. E.; Scullion, M. G.; Krauss, T. F.; Johnson, S. D.,  
34 The electrophotonic silicon biosensor. *Nat. Commun.* **2016**, *7*, 12769.
- 35 31. Flavel, B. S.; Gross, A. J.; Garrett, D. J.; Nock, V.; Downard, A. J., A simple approach to  
36 patterned protein immobilization on silicon via electrografting from diazonium salt solutions.  
37 *ACS Appl. Mater. Interfaces* **2010**, *2* (4), 1184-1190.
- 38 32. Brooksby, P. A.; Downard, A. J., Electrochemical and Atomic Force Microscopy Study  
39 of Carbon Surface Modification via Diazonium Reduction in Aqueous and Acetonitrile  
40 Solutions. *Langmuir* **2004**, *20* (12), 5038-5045.
- 41 33. Page, C. C.; Moser, C. C.; Chen, X.; Dutton, P. L., Natural engineering principles of  
42 electron tunnelling in biological oxidation-reduction. *Nature* **1999**, *402* (6757), 47-52.
- 43 34. Combellas, C.; Kanoufi, F.; Pinson, J.; Podvorica, F. I., Sterically Hindered Diazonium  
44 Salts for the Grafting of a Monolayer on Metals. *J. Am. Chem. Soc.* **2008**, *130* (27), 8576-8577.
- 45 35. Mattiuzzi, A.; Jabin, I.; Mangeney, C.; Roux, C.; Reinaud, O.; Santos, L.; Bergamini, J.-  
46 F.; Hapiot, P.; Lagrost, C., Electrografting of calix[4]arene-diazonium salts to form versatile  
47 robust platforms for spatially controlled surface functionalization. *Nature Communications* **2012**,  
48 *3* (1), 1130.
- 49  
50  
51  
52  
53  
54  
55  
56  
57  
58  
59  
60

- 1  
2  
3 36. Menanteau, T.; Levillain, E.; Breton, T., Electrografting via Diazonium Chemistry: From  
4 Multilayer to Monolayer Using Radical Scavenger. *Chem. Mater.* **2013**, *25* (14), 2905-2909.
- 5 37. Lo, M.; Pires, R.; Diaw, K.; Diariatou, G.-S.; Oturan, M. A.; Aaron, J.-J.; Chehimi, M.  
6 M., Diazonium Salts: Versatile Molecular Glues for Sticking Conductive Polymers to Flexible  
7 Electrodes. *Surfaces* **2018**, *1*, 43-58.
- 8 38. Lo, M.; Diaw, A. K. D.; Gningue-Sall, D.; Aaron, J.-J.; Oturan, M. A.; Chehimi, M. M.,  
9 The role of diazonium interface chemistry in the design of high performance polypyrrole-coated  
10 flexible ITO sensing electrodes. *Electrochem. commun.* **2017**, *77*, 14-18.
- 11 39. Hauquier, F.; Debou, N.; Palacin, S.; Joussetme, B., Amino functionalized thin films  
12 prepared from Gabriel synthesis applied on electrografted diazonium salts. *J. Electroanal. Chem.*  
13 **2012**, *677-680*, 127-132.
- 14 40. Lee, L.; Leroux, Y. R.; Hapiot, P.; Downard, A. J., Amine-terminated monolayers on  
15 carbon: Preparation, characterization, and coupling reactions. *Langmuir* **2015**, *31* (18), 5071-  
16 5077.
- 17 41. Malmos, K.; Dong, M.; Pillai, S.; Kingshott, P.; Besenbacher, F.; Pedersen, S. U.;  
18 Daasbjerg, K., Using a Hydrazone-Protected Benzenediazonium Salt to Introduce a Near-  
19 Monolayer of Benzaldehyde on Glassy Carbon Surfaces. *J. Am. Chem. Soc.* **2009**, *131* (13),  
20 4928-4936.
- 21 42. Nielsen, L. T.; Vase, K. H.; Dong, M.; Besenbacher, F.; Pedersen, S. U.; Daasbjerg, K.,  
22 Electrochemical Approach for Constructing a Monolayer of Thiophenolates from Grafted  
23 Multilayers of Diaryl Disulfides. *J. Am. Chem. Soc.* **2007**, *129* (7), 1888-1889.
- 24 43. Leroux, Y. R.; Fei, H.; Noël, J.-M.; Roux, C.; Hapiot, P., Efficient Covalent Modification  
25 of a Carbon Surface: Use of a Silyl Protecting Group To Form an Active Monolayer. *Journal of*  
26 *the American Chemical Society* **2010**, *132* (40), 14039-14041.
- 27 44. Hudson, J. L.; Jian, H.; Leonard, A. D.; Stephenson, J. J.; Tour, J. M., Triazenes as a  
28 stable diazonium source for use in functionalizing carbon nanotubes in aqueous suspensions.  
29 *Chem. Mater.* **2006**, *18* (11), 2766-2770.
- 30 45. Kongsfelt, M.; Vinther, J.; Malmos, K.; Ceccato, M.; Torbensen, K.; Knudsen, C. S.;  
31 Gothelf, K. V.; Pedersen, S. U.; Daasbjerg, K., Combining Aryltriazenes and Electrogenerated  
32 Acids To Create Well-Defined Aryl-Tethered Films and Patterns on Surfaces. *J. Am. Chem. Soc.*  
33 **2011**, *133* (11), 3788-3791.
- 34 46. Hansen, M. N.; Farjami, E.; Kristiansen, M.; Clima, L.; Pedersen, S. U.; Daasbjerg, K.;  
35 Ferapontova, E. E.; Gothelf, K. V., Synthesis and Application of a Triazene-Ferrocene Modifier  
36 for Immobilization and Characterization of Oligonucleotides at Electrodes. *J. Org. Chem.* **2010**,  
37 *75* (8), 2474-2481.
- 38 47. O'Reilly, J. E., Oxidation-reduction potential of the ferro-ferricyanide system in buffer  
39 solutions. *Biochim Biophys Acta Bioenerg* **1973**, *292* (3), 509-515.
- 40 48. Delincée, H.; Radola, B. J., Fractionation of Horseradish Peroxidase by Preparative  
41 Isoelectric Focusing, Gel Chromatography and Ion-Exchange Chromatography. *Eur. J. Biochem.*  
42 **1975**, *52* (2), 321-330.
- 43 49. Bélanger, D.; Pinson, J., Electrografting: a powerful method for surface modification.  
44 *Chem. Soc. Rev.* **2011**, *40* (7), 3995-4048.
- 45 50. Liu, G.; Liu, J.; Böcking, T.; Eggers, P. K.; Gooding, J. J., The modification of glassy  
46 carbon and gold electrodes with aryl diazonium salt: The impact of the electrode materials on the  
47 rate of heterogeneous electron transfer. *Chem. Phys.* **2005**, *319* (1-3), 136-146.
- 48  
49  
50  
51  
52  
53  
54  
55  
56  
57  
58  
59  
60

- 1  
2  
3 51. Petrangolini, P.; Alessandrini, A.; Berti, L.; Facci, P., An electrochemical scanning  
4 tunneling microscopy study of 2-(6-mercaptoalkyl)hydroquinone molecules on Au(111). *J. Am.*  
5 *Chem. Soc.* **2010**, *132* (21), 7445–7453.
- 6 52. Trammell, S. A.; Lowy, D. A.; Seferos, D. S.; Moore, M.; Bazan, G. C.; Lebedev, N.,  
7 Heterogeneous electron transfer of quinone–hydroquinone in alkaline solutions at gold electrode  
8 surfaces: Comparison of saturated and unsaturated bridges. *J. Electroanal. Chem.* **2007**, *606* (1),  
9 33–38.
- 10 53. Tse, E. C.; Barile, C. J.; Li, Y.; Zimmerman, S. C.; Hosseini, A.; Gewirth, A. A., Proton  
11 transfer dynamics dictate quinone speciation at lipid-modified electrodes. *Phys. Chem. Chem.*  
12 *Phys.* **2017**, *19* (10), 7086–7093.
- 13 54. Heering, H. A.; Weiner, J. H.; Armstrong, F. A., Direct Detection and Measurement of  
14 Electron Relays in a Multicentered Enzyme: Voltammetry of Electrode-Surface Films of *E. coli*  
15 Fumarate Reductase, an Iron–Sulfur Flavoprotein. *J. Am. Chem. Soc.* **1997**, *119* (48), 11628–  
16 11638.
- 17 55. Mooste, M.; Kibena-Pöldsepp, E.; Marandi, M.; Matisen, L.; Sammelselg, V.;  
18 Tammeveski, K., Electrochemical properties of gold and glassy carbon electrodes electrografted  
19 with an anthraquinone diazonium compound using the rotating disc electrode method. *RSC*  
20 *Advances* **2016**, *6* (47), 40982–40990.
- 21 56. Kullapere, M.; Marandi, M.; Matisen, L.; Mirkhalaf, F.; Carvalho, A. E.; Maia, G.;  
22 Sammelselg, V.; Tammeveski, K., Blocking properties of gold electrodes modified with 4-  
23 nitrophenyl and 4-decylphenyl groups. *Journal of Solid State Electrochemistry* **2012**, *16* (2),  
24 569–578.
- 25 57. Cline, K. K.; Baxter, L.; Lockwood, D.; Saylor, R.; Stalzer, A., Nonaqueous synthesis  
26 and reduction of diazonium ions (without isolation) to modify glassy carbon electrodes using  
27 mild electrografting conditions. *Journal of Electroanalytical Chemistry* **2009**, *633* (2), 283–290.
- 28 58. Lee, L.; Brooksby, P. A.; Hapiot, P.; Downard, A. J., Electrografting of 4-  
29 Nitrobenzenediazonium Ion at Carbon Electrodes: Catalyzed and Uncatalyzed Reduction  
30 Processes. *Langmuir* **2016**, *32* (2), 468–476.
- 31 59. Yeap, W. S.; Murib, M. S.; Cuypers, W.; Liu, X.; van Grinsven, B.; Ameloot, M.;  
32 Fahlman, M.; Wagner, P.; Maes, W.; Haenen, K., Boron-Doped Diamond Functionalization by  
33 an Electrografting/Alkyne–Azide Click Chemistry Sequence. *ChemElectroChem* **2014**, *1* (7),  
34 1145–1154.
- 35 60. Kondo, T.; Hoshi, H.; Honda, K.; Einaga, Y.; Fujishima, A.; Kawai, T., Photochemical  
36 Modification of a Boron-doped Diamond Electrode Surface with Vinylferrocene. *J. Phys. Chem.*  
37 *C* **2008**, *112* (31), 11887–11892.
- 38 61. Beamson, G.; Briggs, D., *High Resolution XPS of Organic Polymers : The Scienta*  
39 *ESCA300 Database*. John Wiley and Sons Ltd: Chichester, 1992.
- 40 62. Gengenbach, T. R.; Chatelier, R. C.; Griesser, H. J., Correlation of the Nitrogen 1s and  
41 Oxygen 1s XPS Binding Energies with Compositional Changes During Oxidation of Ethylene  
42 Diamine Plasma Polymers. *Surf. Interface Anal.* **1996**, *24* (9), 611–619.
- 43 63. Singh, K.; Blanford, C. F., Electrochemical Quartz Crystal Microbalance with  
44 Dissipation Monitoring: A Technique to Optimize Enzyme Use in Bioelectrocatalysis.  
45 *ChemCatChem* **2014**, *6* (4), 921–929.
- 46 64. McArdle, T.; McNamara, T. P.; Fei, F.; Singh, K.; Blanford, C. F., Optimizing the Mass-  
47 Specific Activity of Bilirubin Oxidase Adlayers through Combined Electrochemical Quartz  
48  
49  
50  
51  
52  
53  
54  
55  
56  
57  
58  
59  
60

1  
2  
3 Crystal Microbalance and Dual Polarization Interferometry Analyses. *ACS Appl. Mater.*  
4 *Interfaces* **2015**, *7* (45), 25270-25280.

5 65. McNamara, T. P.; Blanford, C. F., A sensitivity metric and software to guide the analysis  
6 of soft films measured by a quartz crystal microbalance. *Analyst* **2016**, *141* (10), 2911-2919.

7 66. Nelson, G. W.; Parker, E. M.; Singh, K.; Blanford, C. F.; Moloney, M. G.; Foord, J. S.,  
8 Surface Characterization and in situ Protein Adsorption Studies on Carbene-Modified Polymers.  
9 *Langmuir* **2015**, *31* (40), 11086-11096.

10 67. Zhang, B.; Sun, L., Artificial photosynthesis: opportunities and challenges of molecular  
11 catalysts. *Chem. Soc. Rev.* **2019**, *48* (7), 2216-2264.

12 68. Ferris, D. P.; McGonigal, P. R.; Witus, L. S.; Kawaji, T.; Algaradah, M. M.; Alnajadah,  
13 A. R.; Nassar, M. S.; Stoddart, J. F., Oxime Ligation on the Surface of Mesoporous Silica  
14 Nanoparticles. *Org. Lett.* **2015**, *17* (9), 2146-2149.

15 69. Larsen, D.; Kietrys, A. M.; Clark, S. A.; Park, H. S.; Ekebergh, A.; Kool, E. T.,  
16 Exceptionally rapid oxime and hydrazone formation promoted by catalytic amine buffers with  
17 low toxicity. *Chem Sci* **2018**, *9* (23), 5252-5259.  
18  
19  
20  
21  
22  
23  
24  
25  
26  
27  
28  
29  
30  
31  
32  
33  
34  
35  
36  
37  
38  
39  
40  
41  
42  
43  
44  
45  
46  
47  
48  
49  
50  
51  
52  
53  
54  
55  
56  
57  
58  
59  
60

## Table of Contents Graphic

